Proc. Natl. Acad. Sci. USA
Vol. 96, pp. 6637–6642, June 1999
Biochemistry

Interfacial membrane docking of cytosolic phospholipase A_2 C2 domain using electrostatic potential-modulated spin relaxation magnetic resonance

ANDY BALL*†, ROBERT NIELSEN*, MICHAEL H. GELB*†‡, AND BRUCE H. ROBINSON*§

Departments of *Chemistry and †Biochemistry, University of Washington, Seattle, WA 98195

Edited by H. Ronald Kaback, University of California, Los Angeles, CA, and approved April 12, 1999 (received for review January 20, 1999)

ABSTRACT **The C2 domain of cytosolic phospholipase A_2 ($C2_{cPLA2}$) plays an important role in calcium-dependent transfer of the protein from the cytosol to internal cellular membranes as a prelude for arachidonate release from membrane phospholipids. By using a recently developed electron paramagnetic resonance approach together with 13 site-specifically nitroxide spin labeled $C2_{cPLA2}$s and membrane-permeant and -impermeant spin relaxants, we have determined the orientation of $C2_{cPLA2}$ with respect to the surface of vesicles of the phospholipid 1,2-dioleoyl-*sn*-glycero-3-phosphomethanol. The structure reveals that the two calcium-binding regions on $C2_{cPLA2}$ that display hydrophobic residues, CBR1 and CBR3, are partially inserted into the core of the membrane. CBR2 that contains predominantly hydrophilic residues is close to the membrane but not inserted. The long axis of the cylindrical $C2_{cPLA2}$ molecule is tilted with respect to the bilayer normal, which brings a cluster of basic protein residues close to the phospholipid headgroups. Such an orientation places the two bound calcium ions close to the membrane surface. All together, the results provide structural support for previous proposals that binding of $C2_{cPLA2}$ to the membrane interface is driven in part by insertion of hydrophobic surface loops into the membrane core. The results are contrasted with previous studies of the interfacial binding of the first C2 domain of synaptotagmin I, which has shorter surface loops that display basic residues for electrostatic interaction with the bilayer surface.**

The C2 domain of cytosolic phospholipase A_2 ($C2_{cPLA2}$) represents a conserved structural motif found in more than 50 proteins involved in lipid signaling, lipid metabolism, and vesicular trafficking (1–5). The function of the C2 domain is mainly to mediate calcium-dependent protein/membrane binding, but reports of C2 domain-dependent protein–protein interactions have also appeared (6, 7). C2 domains comprise a sandwich of two four-stranded antiparallel beta sheets, in what has been described as a Greek key motif (8, 9). Given their structural similarity, the amino acid sequence homology taken across a spectrum of C2 domains from diverse proteins is surprisingly low, with only relatively few amino acids involved in key interactions being conserved. This diversity reflects evolutionary "fine tuning" of the sensitivity of the domain to calcium, the varying requirements of lipid headgroup specificity, and the need to maintain different membrane-protein affinities for different cellular functions.

In cell lysates, cPLA2 transfers to the membrane pellet in the presence of low micromolar amounts of calcium (10). In intact cells, this enzyme transfers from the cytosol to nuclear and endoplasmic reticulum membranes in response to agonists that promote a rise in intracellular calcium (11, 12). This calcium-dependent membrane binding is thought to be mediated by $C2_{cPLA2}$, because this domain shows calcium-dependent membrane binding in the absence of the catalytic domain of cPLA2 (13). Although the isolated catalytic domain is not able to hydrolyze phospholipid substrate presented as vesicles (13), it does contribute to the interfacial binding properties of cPLA2. This is based on the observation that although $C2_{cPLA2}$ requires micromolar calcium to bind to anionic phosphatidylmethanol vesicles, cPLA2 binds to these vesicles in a catalytically productive manner in the absence of calcium (14). The interaction of the catalytic domain of cPLA2 with the membrane is not surprising given that substrate phospholipid has virtually no solubility in the aqueous phase. Evidence has also been presented for the presence of a pleckstrin homology domain as a loop protruding from the catalytic domain of cPLA2, which provides for enhanced interfacial binding to vesicles containing small amounts of phosphatidylinositols (15). Whereas the C2 domain of synaptotagmin shows binding preference to anionic vesicles of phosphatidylserine vs. zwitterionic phosphatidylcholine vesicles (16), $C2_{cPLA2}$ shows the opposite preference (14, 17). However, calcium-dependent affinities of $C2_{cPLA2}$ to anionic phosphatidylmethanol and neutral phosphatidylcholine vesicles are comparable, showing that other factors besides electrostatics contribute to phospholipid headgroup specificity (14).

The mechanism of Ca^{2+}-enhanced binding of $C2_{cPLA2}$ to phosphatidylcholine vesicles is not understood. One model is that Ca^{2+} binding causes a conformational change in $C2_{cPLA2}$ that exposes membrane-inserting protein elements. The crystal structure of $C2_{cPLA2}$ is available only with bound calcium (8), but the x-ray structure of the C2A domain of synaptotagmin I in the presence and absence of three bound calcium ions reveals no major conformational change (18, 19). A second model is that the divalent cation serves as a bridge to coordinate both protein residues and phospholipid headgroups. A third model is that calcium does not coordinate directly to phospholipids but serves only as an electrostatic switch to negate the anionic carboxylate ligands coming from the protein. In the case of C2A of synaptotagmin I, which requires anionic lipids for interfacial binding, such negation would reduce electrostatic repulsion between C2A and anionic phospholipids (19).

The recently determined x-ray and NMR-derived structures of $C2_{cPLA2}$ reveal the presence of three surface loops, also

The publication costs of this article were defrayed in part by page charge payment. This article must therefore be hereby marked "*advertisement*" in accordance with 18 U.S.C. §1734 solely to indicate this fact.

PNAS is available online at www.pnas.org.

This paper was submitted directly (Track II) to the *Proceedings* office. Abbreviations: cPLA2, human cytosolic phospholipase A_2 (group IV phospholipase A_2); $C2_{cPLA2}$, C2 domain of cPLA2 (spin-labeled mutants are designated as A34C-sl, for example, for alanine 34 replaced by spin-labeled cysteine); CBR, calcium-binding region; Crox, tris(oxalato)chromate(III); DOPM, 1,2-dioleoyl-*sn*-glycerol-3-phosphomethanol; EPR, electron paramagnetic resonance; LMV, large multilamellar vesicle.

‡To whom reprint requests should be addressed at: Departments of Chemistry and Biochemistry, Box 351700, University of Washington, Seattle, WA 98195. e-mail: gelb@chem.washington.edu.

§To whom reprint requests should be addressed at: Department of Chemistry, Box 351700, University of Washington, Seattle, WA 98195. e-mail: robinson@chem.washington.edu.

known as calcium-binding regions (CBRs), at one end of the protein that surround the calcium-binding site (8, 20). Two of these loops, CBR1 and CBR2, display hydrophobic residues that may insert into the core of phosphatidylcholine vesicles. Few data are available on the spatial orientation of $C2_{cPLA2}$ at the membrane-aqueous phase interface. Attempts to co-crystallize the C2 domain with bound lipid monomers or phosphocholine headgroups have been unsuccessful (8); soluble 1,2-dibutyryl phosphatidylcholine, phosphocholine, and glycerophosphocholine fail to interfere with the binding of $C2_{cPLA2}$ to micelles (20). We recently developed a technique based on electron paramagnetic resonance (EPR) for determining distances from points on a protein surface to the membrane plane (21). The protein is modified at chosen places by site-specific spin labeling with a nitroxide reagent. The effect of a water-soluble spin-relaxing agent such as tris(oxalato)chromate(III) (Crox) on the relaxation behavior of the spin label is modulated by the concentration of Crox that nitroxide encounters. This concentration depends on the distance of the spin label from the membrane because anionic Crox molecules are electrostatically repelled from the anionic membrane surface (Guoy–Chapman effect). The method can be used to measure distances in the range of 0 to ≈40 Å away from the membrane surface (21). By using an EPR approach developed by Hubbell and coworkers (22), insertion of protein elements into the core of the phospholipid bilayer can also be studied by the site-specific spin-labeling approach. In this case, membrane-embedded nitroxides show enhanced relaxation from lipophilic oxygen molecules. In the present study, we have used EPR spectroscopy and a panel of site-specifically spin-labeled $C2_{cPLA2}$ proteins together with Crox and O_2 relaxing agents to dock $C2_{cPLA2}$ at the membrane-aqueous phase interface.

MATERIALS AND METHODS

Materials. Ni-nitrilotriacetic acid resin is from Qiagen and Q-Sepharose is from Amersham Pharmacia. The spin-labeling reagent (1-oxyl-2, 2, 5, 5-tetramethylpyroline-3-methyl)methanethiosulfonate is from Reanal (Budapest, catalogue no. HO-225). DTT (Ultrapure) is from United States Biochemical. 1,2-Dioleoyl-*sn*-glycero-3-phosphomethanol (DOPM) is from Avanti Polar Lipids. Crox was prepared as described (21).

Site-Directed Mutagenesis. The original $C2_{cPLA2}$ expression construct was kindly provided by R. Williams (University of Cambridge) (14) and produces bacterial expression of residues 16–141 of human $C2_{cPLA2}$ containing the short N-terminal extension $MRGSH_6GLVPRGS$ to facilitate purification. *Escherichia coli* strain BL21-(DE3) (Novagen) was used for protein production. Plasmid DNA was purified from small-scale cultures by using Qiagen mini-prep columns. Codons for cysteine were introduced by using the QuickChange kit from Stratagene.

Expression, Refolding, Spin Labeling, and Purification of $C2_{cPLA2}$ Mutants. Bacteria was cultured in 4 liters of Luria broth with 60 μg/ml ampicillin. When the culture reached an OD_{600} of 0.5, protein expression was induced with 1 mM isopropyl-β-D-thiogalactopyranoside for 5 hr. Cells were pelleted at 3,000 × *g*, suspended in 30 ml of ice-cold lysis buffer (50 mM Tris·HCl, pH 8.0/1 mM EDTA/1 mM EGTA/5 mM benzamidine/3 mM freshly added DTT/1 mM freshly added phenylmethylsulfonyl fluoride), and disrupted by sonication on ice. Inclusion bodies were pelleted by centrifugation at 3,000 × *g* at 4°C, and the pellet was washed with 30 ml of ice-cold lysis buffer. After a final spin, the inclusion body pellet was incubated with high urea buffer (20 mM Tris·HCl/8 M urea/100 mM ammonium chloride/3 mM DTT, pH 7.4) for 2 hr at room temperature with gentle shaking. Insoluble material was removed by centrifugation at 12,000 × *g* for 10 min at 4°C.

The clarified supernatant was mixed with 5 ml of Ni-nitrilotriacetic acid (NTA) agarose, and the mixture was periodically mixed by inversion for 1 hr at room temperature before being poured into a column (2.5 cm i.d.). The resin was washed with 15 column volumes of high urea buffer (gravity flow). The resin in the column was immediately resuspended in 20 ml of refolding buffer (50 mM Tris·HCl/1.5 M urea/3 mM DTT, pH 7.2) and kept suspended by occasional inversion for 1 hr at room temperature. Ten column volumes of refolding buffer were passed through the column before a final wash with 50 ml of 50 mM Tris·HCl, pH 7.5. The protein was eluted from the column by using 50 mM Tris·HCl, 300 mM imidazole, pH 7.5, and the protein concentration immediately assessed by using the Bradford assay (Bio-Rad). This extensive washing served to ensure complete removal of DTT just before spin labeling. To the eluted protein was immediately added 1 mol equivalent of spin-labeling reagent from a 30 mM stock in acetonitrile and the mixture incubated on ice for 30 min. This labeling step was repeated twice. Although $C2_{cPLA2}$ could also be refolded in solution, the resin-bound method avoids the lengthy process of dialysis into refolding buffer or the concentration of protein solution after dilution of denatured protein into buffer without denaturatant. Also, removal of DTT from protein bound to Ni-NTA is rapid, which avoids potential intermolecular disulfide formation before spin labeling.

Correctly refolded protein was separated from denatured material and free spin label by using a 3 ml Q-Sepharose column. After spin labeling, the material was loaded onto the column in the labeling buffer and the column washed with 30 column volumes of 50 mM Tris·HCl, pH 7.5, to completely remove free spin label. The column was developed with a salt gradient (0–1 M NaCl, total volume 180 ml) at a flow rate of 3 ml/min to elute the refolded and spin-labeled protein at approximately 130 mM NaCl (denatured protein, when present, eluted at approximately 500 mM NaCl). A portion of purified protein (0.25 ml of the Q-Sepharose pool) was desalted by using a spin column of P6 gel (Bio-Rad, 1 ml in a 1-ml tuberculin syringe) and concentrated 5- to 10-fold by using a SpeedVac (Savant). The Tris·HCl, pH 7.5, buffer for the spin column was chosen so that the final buffer concentration is 50 mM after protein concentration. Final protein concentration ranged from 1–3 mg/ml (Bradford assay). All proteins were >95% pure as assessed by SDS/PAGE on a 16% gel. In most refolding runs, the amount of denatured protein was <5% of the total.

Calcium-dependent interfacial binding of each spin-labeled $C2_{cPLA2}$ mutant was examined essentially as described (23). Assays were performed in 50 mM Tris·HCl, pH 7.5/150 mM NaCl/2 mM EGTA with and without 2.3 mM $CaCl_2$. DOPM from a 50 mg/ml stock in chloroform was dried down under a nitrogen stream. The residue was resuspended in assay buffer as large multilamellar vesicles (LMVs) at 1 mg/ml by vigorous vortexing over ≈3 min to give an opalescent suspension. Binding samples contained 5 μg protein in 300 μl assay buffer with 100 μl vesicle stock. After incubation at room temperature for 15 min, LMVs were pelleted in a microfuge at 10,000 × *g* for 15 min. Samples of the pellet and supernatant were resolved on a 15% SDS/PAGE gel. For some proteins [wild type, mutant with Leu-39 replaced with spin-labeled Cys (L39C-sl), E88C-sl, S110C-sl, Q126C-sl, C139-sl], binding was examined with different calcium concentrations (0, 0.2, 0.5, 1, 5, 10, 20, 50, and 1,000 μM). A calcium–EGTA buffer was used to generate free calcium in the 0- to 10-μM range, and $CaCl_2$ in excess of EGTA was used to generate 20–1,000 μM free calcium (14). For some proteins (wild type, A34C-sl, D55C-sl, E88C-sl, Q126C-sl), calcium-dependent partitioning into Triton X-114-rich phase was assessed as described (23).

EPR Studies. Large unilamellar vesicles of DOPM were prepared from a 50 mg/ml stock of DOPM in chloroform. After removal of solvent with a stream of N_2, lipid residue was resuspended in 50 mM Tris·HCl, pH 7.5, to give a lipid concentration of 200 mM, and the suspension was subjected to multiple freeze–thaw cycles followed by extrusion through a 0.1-μm filter (24). To prepare vesicle-containing EPR sample,

8 μl of spin-labeled $C2_{cPLA2}$ stock (1–3 mg/ml), 10 μl of DOPM large unilamellar vesicles stock, and 2 μl of calcium-containing buffer with or without Crox were combined in an Eppendorf tube. The final buffer components are 50 mM Tris·HCl, pH 7.5, 0.3 mM $CaCl_2$, and with or without 10 mM Crox. EPR samples in the absence of lipid were made with 18 μl protein stock and 2 μl calcium-containing buffer with or without Crox (final concentrations, 50 mM Tris·HCl, 0.3 mM CaCl2, ±10 mM Crox). EPR samples (3 μl) were contained in wax (Critoseal)-plugged Teflon capillary tubes (24 light wall, Zeus, Orangeburg, SC), which allowed for gas exchange in <20 min at 21°C. EPR spectra were acquired with a loop-gap resonator at a field resolution of 0.125 G per point and were averaged three times (25, 26). Samples without oxygen were collected by flowing 99% N_2 through the sample chamber, and oxygen was introduced by flowing medical air (21% O_2).

The nonlinear Poisson–Boltzmann equation is used to calculate the concentration of Crox as a function of distance normal to the membrane (described below). The equation contains a term that depends on the concentration of all electrolytes in solution. To maintain electric neutrality, the anionic lipids that make up the electrostatic planar membrane need to be included to balance the counter ions present in solution, and yet these lipid anions affect the electrostatic potential differently than do ions in solution. Thus, the Poisson–Boltzmann equation was solved with and without the inclusion of anionic lipid and its counter ion. The Euler angles and displacement distance for the orientation of $C2_{cPLA2}$ with respect to the membrane for the two solutions changed by less than the errors in these values, which are given in *Results*.

Molecular Modeling and EPR-Based Docking. Suitable sites for mutagenesis were identified by using the crystal structure of $C2_{cPLA2}$ (8). Side chains were selected that point out from the bulk of the protein. The spin label was grafted onto $C2_{cPLA2}$ in such a way as to avoid steric clashes with adjacent protein residues. Six of thirteen spin-labeled proteins fitted into either one or the other of two preferred conformations, as seen in the x-ray structures of T4 lysozyme labeled with the same spin-labeling reagent (R. Langen, K.-J. Oh, H. McHaourab, K. Hideg, W. L. Hubbell, personal communication). These are defined by dihedral angles of −60, −60, −90, or −180, −90, −90 for the C_α-C_β, C_β-S_γ, and S_γ-S_δ bonds (using the standard angle conventions). The remaining spin labels were fitted in such a way as to avoid clashes with adjacent protein residues while preserving the −90 dihedral angle of the S_γ-S_δ bond. The Cartesian coordinates of the nitroxide nitrogen were used for $C2_{cPLA2}$/membrane-docking analysis (see below).

$C2_{cPLA2}$ was docked to DOPM membranes by rigid protein body movement to obtain the best fit of experimental and modeled values of Φ (defined below). Two Euler angles and the displacement distance of protein from the membrane were varied by using the Marquardt–Levenberg search algorithm programmed in MATLAB (Mathworks, Natick, MA). A third Euler angle is not needed because the membrane is of infinite extent. To account for the finite range of excursion of the nitroxide (as evidenced by the low-order parameters in the EPR spectra) and the finite size of the Crox (≈4 Å diameter), the electrostatic potential $\Psi(r)$ was convoluted with a 5-Å-wide Gaussian. It may be noted that values of z_{crox} and $\Psi(0)$ and a convolution over $\Psi(r)$ affected only the protein–membrane distance and did not alter the protein–membrane rotational orientation (the definition of all numerical quantities is given below).

RESULTS

Preparation of Functional Spin-Labeled $C2_{cPLA2}$ Proteins. Thirteen single-site $C2_{cPLA2}$ mutants were prepared in which a surface-exposed residue was replaced with cysteine. Mutation sites were selected to provide near-uniform coverage of $C2_{cPLA2}$. L39C-sl (Leu-39 replaced with spin-labeled Cys) and A34C-sl are on the external face of a short helix that constitutes Ca^{2+}-binding loop 1 (CBL1), and V97C-sl is on CBL3. Residues that run around the circumference of the $C2_{cPLA2}$ cylinder and about halfway down the length of the cylinder were mutated (R61C-sl, V70C-sl, E88C-sl, Q126C-sl). Finally, a ring of residues were mutated at the end of the cylinder opposite the Ca^{2+}-binding end (D55C-sl, A78C-sl, S110C-sl, K113C-sl, K117C-sl, C139-sl).

The tryptophan emission spectra of all spin-labeled $C2_{cPLA2}$s were virtually identical to that of the wild-type protein, and they showed the characteristic shift in emission maximum reported for the unfolded-to-folded transition (17). Wild-type $C2_{cPLA2}$ and spin-labeled mutants displayed a similar degree of calcium-induced partitioning into Triton X-114-rich buffer phase (not shown) (23). Calcium-dependent binding of spin-labeled $C2_{cPLA2}$s to LMVs of DOPM was assessed by monitoring the amount of protein left in the supernatant after pelleting the vesicles by centrifugation in the absence and presence of 300 μM free calcium. Wild-type protein and all 13 spin-labeled mutants showed >95% binding to DOPM LMVs in the presence of calcium and little (<5%) binding in the absence of calcium (not shown). For six of the proteins (see *Methods*), the calcium dependence of binding was studied with different calcium concentrations. The concentration of free calcium required for 50% of the protein to bind to DOPM LMVs ranged from 8 to 15 μM (not shown). All together, these results strongly argue that spin labeling of $C2_{cPLA2}$ does not significantly perturb calcium-dependent binding of $C2_{cPLA2}$ to anionic DOPM vesicles.

EPR-Based Docking of $C2_{cPLA2}$ on Membranes. We recently developed an EPR method for determining the distance of a protein surface-bound nitroxide spin label to the planar surface of an anionic phospholipid membrane (21). In this approach, the effect of the spin-relaxing agent Crox on the relaxation of the nitroxide spin is measured in the presence and absence of vesicles of the anionic phospholipid DOPM. Previous work showed that $C2_{cPLA2}$ binds to DOPM vesicles in a calcium-dependent manner with a K_{Ca} of 5 μM (14). Crox molecules have a charge of −2.3 (W. L. Hubbell, personal communication) and are electrostatically repelled from the surface of DOPM vesicles according to the Poisson–Boltzmann equation (equation 7 of ref. 21). The relaxation of the protein-bound nitroxide depends on the rate of collision of Crox with nitroxide, which in turn depends on the concentration of Crox in the vicinity of the spin label. Because the latter is a function of the distance normal to the membrane surface, the method provides a measure of the spin label–membrane distance. As discussed previously in detail (21), this method of protein–membrane docking can be problematic if the protein undergoes a conformational change on membrane binding that modifies the structure of the protein in the vicinity of the nitroxide to the point that the nitroxide–Crox collision frequency is altered in ways other than electrostatic repulsion of Crox by the membrane. In the absence of such a conformational change, the effect of the local electrostatic potential from the protein at the spin-label site on Crox collision is accounted for by measuring the EPR parameters for protein both in solution and bound to membranes (21), as presented below.

For each spin-labeled mutant, the peak-to-peak height of the central line of the first derivative EPR spectrum of spin-labeled $C2_{cPLA2}$ is measured as function of the power of microwave radiation incident on the sample, and the data are fit to the power rollover equation to obtain the parameter P_2, which depends on the properties of the nitroxide (21) (an example set of curves and data for all mutants are published as supplemental data on the PNAS web site, www.pnas.org). The quantity ΔP_2 is defined as the difference in P_2 values in the presence and absence of Crox and is directly proportional to the concentration of Crox in the vicinity of the spin labeled (21). ΔP_2 is measured in the presence and absence of DOPM vesicles to obtain the shielding factor, Φ (Table 1), which varies from 0 (membrane completely shields the nitroxide from relaxation by Crox) to 1 (membrane has no effect) (21).

Table 1. Exposure factors

Site	Φ*	Site	Φ*
A34	0.04 ± 0.01	V97	0.02 ± 0.02
L39	0.00 ± 0.02	S110	0.61 ± 0.02
D55	0.06 ± 0.02	K113	0.27 ± 0.03
R61	0.155 ± 0.005	K117	0.75 ± 0.05
V70	0.53 ± 0.02	Q126	0.12 ± 0.02
A78	0.186 ± 0.006	C139	0.36 ± 0.01
E88	0.23 ± 0.02		

*Φ, as calculated by equation 5 of ref. 21.

Theoretical shielding factors were calculated by using the nonlinear Poisson–Boltzmann equation and a membrane surface potential of −77 ± 3 mV (21). To orient $C2_{cPLA2}$ with respect to the surface of DOPM large unilamellar vesicles, it was assumed that the x-ray structure of $C2_{cPLA2}$ (8) is maintained when the protein binds to membranes and that the membrane that contacts the enzyme is planar. Regression analysis was carried out by varying the protein-to-membrane distance and the two Euler angles for the rigid-body rotation of $C2_{cPLA2}$ about its center. Several trials were executed with systematic variation of the initial conditions. In all cases, the analysis converged to a single $C2_{cPLA2}$-membrane orientation. Fig. 1 shows the fit of experimental Φ to calculated Φ. Except for the values of Φ for E88C-sl and S110C-sl, all of the experimental Φ values well fit the theoretical curve predicted by the modeled orientation (solid line). The fit shown in Fig. 1 does not include data for E88C-sl and S110C-sl. If data for these two mutants are not included, the Euler angles for protein–membrane orientation are 58 ± 2 and 186 ± 2 degrees (note: the absolute values of the Euler angles are in a reference frame used for our submitted Protein Data Bank file), and the error in the displacement distance is 0.4 Å. If these two mutants are included, the Euler angles are 63 ± 7 and 194 ± 8 degrees, and the displacement distance increases by 2 Å. Such numbers indicate that the orientation of $C2_{cPLA2}$ at the membrane is well determined by the use of many more spin-labeled mutants than the minimum of three needed. Fig. 2 shows the best-fit orientation of $C2_{cPLA2}$ with respect to the DOPM membrane plane based on results shown in Fig. 1.

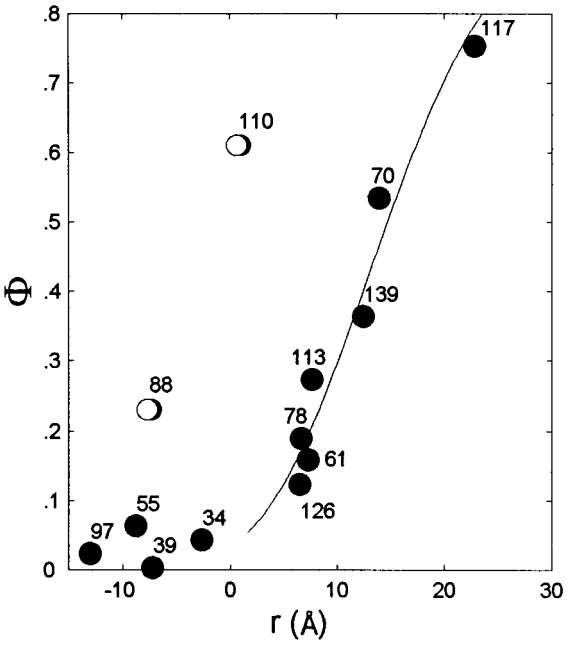

FIG. 1. Regression analysis of the $C2_{cPLA2}$-membrane orientation. The solid line shows values of simulated Φ obtained by using the nonlinear Poisson–Boltzmann equation as a function of distance from the spin label nitrogen to the membrane (r). The circles are the values of Φ calculated from the experimental EPR data as a function of the modeled distance from the spin label to the membrane for each residue (the residue number is shown next to each circle). Residues 34, 39, 55, and 97 are all close to the membrane, and those that penetrate the interior of the bilayer were distinguished by the oxygen effect (see text).

Values of Φ for A34C-sl, L39C-sl, D55C-sl, and V97C-sl are very close to zero. According to the modeled orientation, these residues penetrate to different extents into the interior of the bilayer (negative values of r). Hubbell and coworkers have shown that the efficiency of relaxation of a protein-bound nitroxide by molecular oxygen increases as the spin label's position is shifted toward the center of the bilayer (22). This is because the concentration of hydrophobic oxygen molecules is highest at the center of the bilayer and continuously drops toward the bulk aqueous phase concentration moving toward the phospholipid-water boundary. Thus, we obtained power rollover curves in the presence and absence of O_2 and DOPM (analogous to Fig. 1 with O_2 replacing Crox). Of the five mutants tested for O_2-dependent relaxation (A34C-sl, L39C-sl, D55C-sl, V70C-sl, and V97C-sl), L39C-sl and V97C-sl show the biggest O_2 effect. In the absence of DOPM, the presence of O_2 increases P_2 by 0.097 ±.002 G^2 for L39C-sl and by 0.085 ±.005 G^2 for V97C-sl. In the presence of membranes, P_2 increases by 0.189 ± 0.01 G^2 and 0.23 ± 0.01 G^2 for L39C-sl and V97C-sl, respectively. In contrast, for V70C-sl and D55C-sl, P_2 increases by the same amount, 0.12 ± 0.05 and 0.16 ± 0.05, respectively, when O_2 is added in the absence and presence of DOPM. A34C-sl shows intermediate O_2 sensitivity, ΔP_2 = 0.107 ± 0.006 and 0.131 ± 0.007 in the absence and presence of DOPM, respectively. Thus, V70C-sl and D55C-sl spin labels are not inserted into the membrane core. V97C-sl spin label is inserted the most followed by L39C-sl and then A34C-sl spin labels. These trends agree with the docked structure of $C2_{cPLA2}$ on DOPM vesicles (Fig. 1) and provide strong support for the partial insertion of this protein into the interior of the bilayer.

The reason for the anomalous behavior of E88C-sl and S110C-sl is unknown. An acceptable regression fit of experimental and theoretical values of Φ can be obtained by using these two spin labels together with R61C-sl (which lies on the same β-sheet as E88C-sl and S110C-sl) and with those mutants that have values of Φ close to zero (A34C-sl, L39C-sl, D55C-sl, and V97C-sl). R61C-sl and V70C-sl fit both models well, but K113C-sl and Q126C-sl and to some extent A78C-sl and C139-sl are not well included in the new fit. The problem with this orientation is that it positions A34C-sl above the membrane, which is inconsistent with the O_2 relaxation data showing penetration of this residue into the membrane. Fig. 3 compares this alternative protein–membrane orientation to that based on the fit shown in Fig. 1. The two orientations are very similar, differing only slightly in the tilt of the long axis (24°) of the cylindrical $C2_{cPLA2}$ molecule with respect to the membrane normal.

Description of Membrane-Docked $C2_{cPLA2}$. The structural features of the $C2_{cPLA2}$-membrane orientation shown in Fig. 2 are summarized as follows. The long axis of the protein cylinder composed of an anti-parallel β-sandwich of two four-stranded sheets is significantly tilted away from the membrane normal such that the face of the molecule containing β-strands 2, 3, 5, and 6 comes close to the membrane plane (β-strand numbers as reported ref. 8). Such a tilt brings the cluster of basic residues on β-strand 3, especially R57 and R59, close to the membrane surface such that electrostatic attraction of these residues with the anionic phosphate groups of membrane phospholipids may be possible.

C2 domains including $C2_{cPLA2}$ contain three calcium-binding regions (CBR1, CBR2, CBR3). These regions are composed of surface loops that connect sequential β-strands and that form the walls of the cavity where the two calciums sit. CBR1 of $C2_{cPLA2}$ is the longest loop and includes a short α-helix that displays hydrophobic residues F35, M38, and L39 on the same face and pointing away from the calcium-binding sites. The membrane-

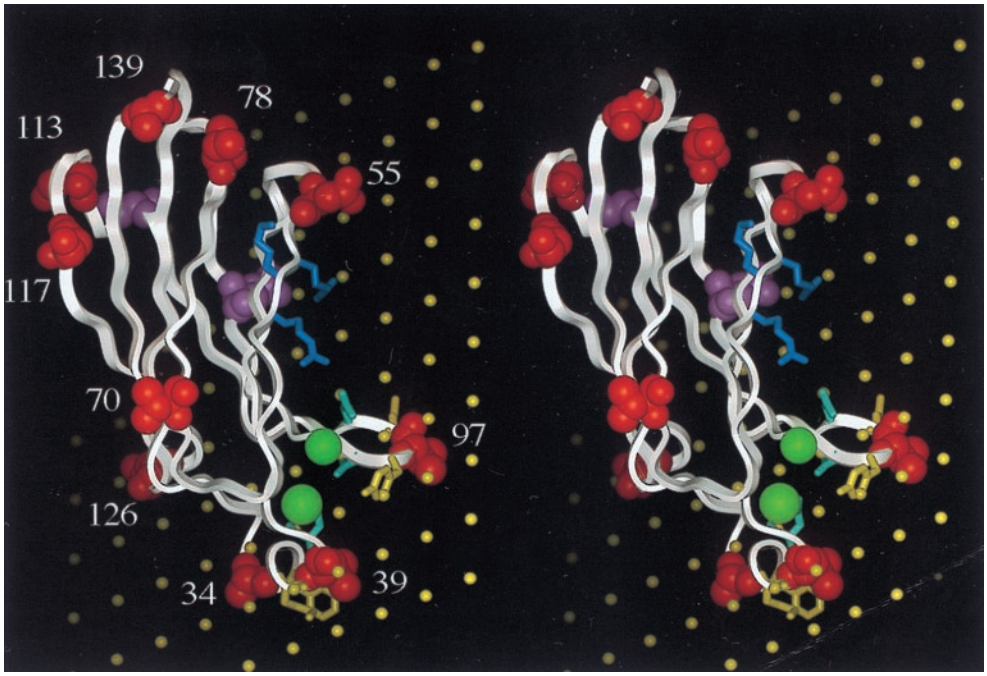

FIG. 2. Stereoview of EPR-based docked $C2_{cPLA2}$ on DOPM membranes by using the data in Fig. 1. The position of the protein with respect to the membrane (plane of electrostatic potential −77 mV, shown as an array of yellow balls 6 Å apart) is as shown in Fig. 2. The protein backbone is shown as a white ribbon, and native residues that were replaced with spin labels are shown as van der Waals surfaces in red except for residues 88 and 110, which are shown in pink. The two calcium ions are shown as green spheres. CBR1 contains residues 34 and 39 and also F35 and M38 (shown as yellow sticks) and D40 (cyan stick). CBR3 contains V97 and also Y96 and M98 (yellow sticks) and N95 and D99 (cyan sticks). Basic residues R57, K58, and R59 are shown as blue-gray sticks.

docked structure clearly indicates that this loop penetrates into the interior of the membrane. Flanking this stretch of hydrophobics in CBR3 is A34 and D40, which sit close to the membrane but do not penetrate the lipid core. The β-carboxylate of D40 donates ligands to both calcium ions. CBR3 is also penetrated into the membrane. It contains membrane-inserted hydrophobic residues Y96, V97, and M98, flanked by hydrophilic residues N95 and D99, which are not inserted. The β-carbonyl of N95 is in the direct coordination sphere of one of the calcium ions. The remaining surface loop CBR2 is not inserted into the membrane. This is perhaps not surprising because this loop displays hydrophilic residues N64, N65, and D66. The β-carbonyl of N65 is a ligand to one of the bound calcium ions.

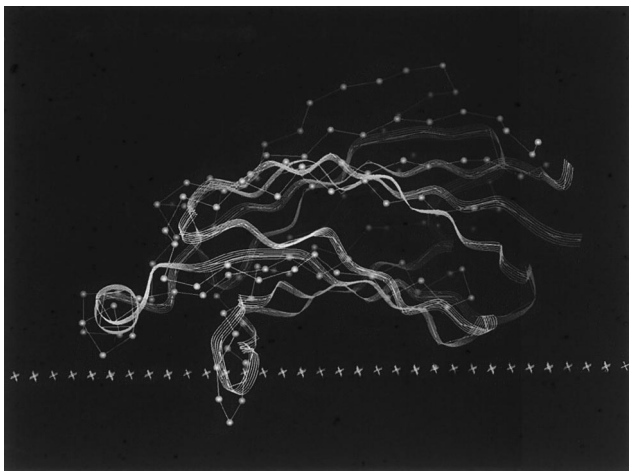

FIG. 3. Comparison of the optimal $C2_{cPLA2}$-membrane orientation (given by the fit in Fig. 1, ribbon diagram), which excludes data from residues 88 and 110, to that given by the alternative regression fit described in the text (ball-and-stick diagram). The membrane planes of the two docked structures are superimposed and shown edge on as a row of crosses.

Equilibrium dialysis experiments indicate that $C2_{cPLA2}$ binds two calcium ions in the presence and absence of a membrane interface (27), which is consistent with x-ray crystallographic and microcalorimetry studies for the protein in the aqueous phase (8, 20). The two calcium ions contain bound waters that could be replaced by coordination of the phosphate headgroups of membrane phospholipids. Calcium I has six ligands, two of which are waters, and calcium II has seven ligands, one of which is water (8). In the docked $C2_{cPLA2}$-membrane structure, the two calciums are facing the membrane and could bind a phospholipid molecule, with some displacement of the phospholipid from the plane of the bilayer being required. The EPR studies do not directly bear on the issue of calcium–phospholipid coordination.

DISCUSSION

The EPR-based spin relaxation method used here to dock $C2_{cPLA2}$ on the membrane surface when carried out with a dozen or so spin-labeled sites gives an orientation of the protein with the membrane plane to within 2° for the Euler angles. By using a collection of spin labels placed over the entire surface of the protein, any error in docking orientation originating from the uncertainty in local conformation of the nitroxide-labeled cysteine is minimized (21). The displacement distance of the protein from the membrane, but not the Euler angles, determined from the data by using Crox is less accurate because its evaluation depends on knowing the surface electrostatic potential of the anionic membrane surface and the charge on Crox. Also the concentration of Crox very near the surface may not be well described by the simple electrostatic Poisson–Boltzmann theory, and Crox is not a point charge. Thus, all spin labels within perhaps a few angstroms of the membrane surface will yield values of Φ close to zero. The orientation of the protein with respect to the membrane is determined mainly from a number of intermediate spin label–membrane distances (Fig. 1). Supplementing the EPR relaxation data obtained with Crox with O_2-dependent studies is a powerful method for better estimation

of the protein–membrane displacement distance. Enhanced O_2-spin label relaxation by binding of $C2_{cPLA2}$ to membranes provides strong evidence for the insertion of specific residues into the membrane core, in particular those on the external surfaces of CBR1 and CBR3.

The $C2_{cPLA2}$-membrane orientation is similar in many ways to that proposed by Perisic *et al.,* who determined the x-ray structure of $C2_{cPLA2}$ containing two bound calcium ions (8). In this earlier study, $C2_{cPLA2}$ was docked against the membrane such that CBR1 and CBR3 are inserted into the membrane and tilted down toward the membrane to bring the patch of basic residues (57–59) close to the phospholipid head groups. This tilting of the long axis of the $C2_{cPLA2}$ cylinder with respect to the membrane normal has been directly demonstrated in our EPR study. The C2B domain of synaptotagmin IV also contains a cluster of basic residues on β-strand 3, and mutation of these residues abolishes binding to inositol tetrakisphosphate, suggesting that this protein region contributes to binding to phosphatidylinositol phosphate-containing vesicles (28).

The insertion of CBR1 and CBR3 into the interior of the membrane is consistent with the prevalence of surface-exposed hydrophobic residues on these loops. The hydrophobic residues of CBR1 and CBR3 as well as the residues that flank the hydrophobic segments are conserved among cPLA2s from eight species, including nonmammalian species. In marked contrast, synaptotagmin I C2A domain contains a much smaller CBR1 loop that probably cannot insert into the membrane very much. The hydrophobic residues Y96, V97, and M98 of CBR3 of $C2_{cPLA2}$ are replaced by R, S, and K, respectively, in CBR3 of synaptotagmin I C2A, suggesting that surface-exposed side chains of CBR3 of the latter contact the phospholipid headgroups rather than insert into the core of the membrane. These suggestions are supported by the observation that synaptotagmin I C2A but not $C2_{cPLA2}$ membrane binding is greatly enhanced by the presence of anionic phospholipids and by the fact that dissociation of C2A but not $C2_{cPLA2}$ from membranes occurs with high salt. Also, $C2_{cPLA2}$, but not C2A, is covalently modified by a membrane-residing photolabeling reagent, which supports a membrane-penetration model (23). Consistent with the insertion of hydrophobic surface loops of $C2_{cPLA2}$ into the membrane is the observation that this protein binds tighter to phosphatidylcholine vesicles than to those made of phosphatidylserine (14, 15, 17). However, this is not solely caused by an electrostatic effect, because the affinity of $C2_{cPLA2}$ for anionic phosphatidylmethanol vesicles is comparable to that for phosphatidylcholine (14). Perhaps the much smaller headgroup of phosphatidylmethanol vs. phosphatidylcholine facilitates insertion of the hydrophobic surface loops into the core of the membrane, and this offsets the unfavorable electrostatic interactions between $C2_{cPLA2}$ and phosphatidylmethanol vesicles. Phosphatidylserine, which contains a bulky and anionic headgroup, would not support binding of $C2_{cPLA2}$. Monolayer surface pressure studies show that cPLA2 penetrates into the monolayer much more than secreted PLA2s (29), which is consistent with the present EPR studies for $C2_{cPLA2}$ and those for bee venom-secreted PLA2 (21).

The solution structure of $C2_{cPLA2}$ has been determined by NMR, and a model for the membrane-binding surface has been proposed based on changes in ^{15}N chemical shift on binding of the protein to micelles of dodecylphosphorylcholine (20). The largest shift changes occur for residues in CBR1 and CBR3, which supports a change in environment as residues in these loops insert into micelles. Residues in CBR2 are shifted to a lesser extent. These trends are consistent with our membrane-docked $C2_{cPLA2}$ structure. NMR studies also show that calcium binding to $C2_{cPLA2}$ in the presence and absence of membranes does not cause major conformational changes in the protein (20).

A key issue that remains to be settled is the mechanism of calcium-induced $C2_{cPLA2}$ membrane binding. The equilibrium constant for dissociation of Ca^{2+} from $C2_{cPLA2}{\cdot}Ca^{2+}$ in the aqueous phase is only ≈10-fold larger than the value in the presence of saturating phosphatidylcholine vesicles (14, 27). This indicates that saturating calcium enhances the binding of $C2_{cPLA2}$ to phosphatidylcholine by ≈10-fold, which is consistent with an ≈10-fold increase in the concentration of phosphatidylcholine vesicles required to drive the protein onto the membranes in the absence vs. presence of calcium (14). Thus, the presence of calcium enhances membrane binding of $C2_{cPLA2}$ by only ≈1.3 kcal/mol. The fact that binding of calcium to $C2_{cPLA2}$ in the water layer promotes protein partitioning to a more hydrophobic Triton X-114-rich phase shows that calcium binding increases the hydrophobicity of the protein's surface, possibly by changing the net charge of the calcium-binding region from −3 for apo-$C2_{cPLA2}$ to +1 for the complex with two bound calciums (23).

Note Added in Proof. After acceptance of this paper for publication, the x-ray structure of full-length cPLA2 appeared (30). The orientation of $C2_{cPLA2}$ with respect to the membrane predicted to position the active site against the membrane appears very similar to our EPR-determined orientation.

We are grateful to R. Williams and J. Clark for providing bacterial expression systems for $C2_{cPLA2}$ and to E. Nalefski for helpful discussions.

1. Nalefski, E. A. & Falke, J. J. (1996) *Protein Sci* **5,** 2375–2390.
2. Wymann, M. P. & Pirola, L. (1998) *Biochim. Biophys. Acta* **1436,** 127–150.
3. Plant, P. J., Yeger, H., Staub, O., Howard, P. & Rotin, D. (1997) *J. Biol. Chem.* **297,** 32329–32336.
4. Ibata, K., Fukuda, M. & Mikoshiba, K. (1998) *J. Biol. Chem.* **273,** 12267–12273.
5. Rizo, J. & Sudhof, T. C. (1998) *J. Biol. Chem.* **273,** 15879–15882.
6. Chapman, E. R., Desai, R. C., Davis, A. F. & Tornehl, C. K. (1996) *J. Biol. Chem.* **271,** 5844–5849.
7. Sugita, S., Hata, Y. & Sudhof, T. C. (1996) *J. Biol. Chem.* **271,** 1262–1265.
8. Perisic, O., Fong, S., Lynch, D. E., Bycroft, M. & Williams, R. L. (1998) *J. Biol. Chem.* **273,** 1596–1604.
9. Grobler, J. A. & Hurley, J. H. (1997) *Nat. Struct. Biol.* **4,** 261–262.
10. Channon, J. Y. & Leslie, C. C. (1990) *J. Biol. Chem.* **265,** 5409–5413.
11. Glover, S., de Carvalho, M., Bauburt, T., Jonas, M., Chi, E., Leslie, C. C. & Gelb, M. H. (1995) *J. Biol. Chem.* **270,** 15359–15367.
12. Schievella, A. R., Regier, M. K., Smith, W. L. & Lin, L. L. (1995) *J. Biol. Chem.* **270,** 30749–30754.
13. Nalefski, E. A., Sultzman, L. A., Martin, D. M., Kriz, R. W., Towler, P. S., Knopf, J. L. & Clark, J. D. (1994) *J. Biol. Chem.* **269,** 18239–18249.
14. Hixon, M. S., Ball, A. & Gelb, M. H. (1998) *Biochemistry* **37,** 8516–8536.
15. Mosior, M., Six, D. A. & Dennis, E. A. (1998) *J. Biol. Chem.* **273,** 2184–2191.
16. Shao, X., Fernandez, I., Sudhof, T. C. & Rizo, J. (1998) *Biochemistry* **37,** 16106–16115.
17. Nalefski, E. A., McDonagh, T., Somers, W., Seehra, J., Falke, J. J. & Clark, J. D. (1998) *J. Biol. Chem.* **273,** 1365–1372.
18. Ubach, J., Zhang, X., Shao, X., Sudhof, T. C. & Rizo, J. (1998) *EMBO J.* **17,** 3921–3930.
19. Zhang, X., Rizo, J. & Sudhof, T. C. (1998) *Biochemistry* **37,** 12395–12403.
20. Xu, G. Y., McDonagh, T., Yu, H. A., Nalefski, E. A., Clark, J. D. & Cumming, D. A. (1998) *J. Mol. Biol.* **280,** 485–500.
21. Lin, Y., Nielsen, R., Murray, D., Mailer, C., Hubbell, W. L., Robinson, B. H. & Gelb, M. H. (1998) *Science* **279,** 1925–1929.
22. Altenbach, C., Greenhalgh, D. A., Khorana, H. G. & Hubbell, W. L. (1994) *Proc. Natl. Acad. Sci. USA* **91,** 1667–1671.
23. Davletov, B., Perisic, O. & Williams, R. L. (1998) *J. Biol. Chem.* **273,** 19093–19096.
24. Bayburt, T. & Gelb, M. H. (1997) *Biochemistry* **36,** 3216–3231.
25. Mailer, C., Danielson, S. J. & Robinson, B. H. (1985) *Rev. Sci. Instrum.* **56,** 1917–1925.
26. Mailer, C., Haas, D. A., Hustedt, E. J., Gladden, J. G. & Robinson, B. H. (1991) *J. Magn. Reson.* **91,** 475–496.
27. Nalefski, E. A., Slazas, M. M. & Falke, J. J. (1997) *Biochemistry* **36,** 12011–12018.
28. Fukuda, M., Kojima, T., Aruga, J., Niinobe, M. & Mikoshiba, K. (1995) *J. Biol. Chem.* **270,** 26523–26527.
29. Lichtenbergova, L., Yoon, E. T. & Cho, W. (1998) *Biochemistry* **37,** 14128–14136.
30. Dessen, A., Tang, J., Schmidt, H., Stahl, M., Clark, J. D., Seehra, J. & Somers, W. S. (1999) *Cell* **97,** 349–360.